Available online at www.sciencedirect.com

ScienceDirect

Procedia Engineering 81 (2014) 1408 – 1413

Procedia Engineering

www.elsevier.com/locate/procedia

11th International Conference on Technology of Plasticity, ICTP 2014, 19-24 October 2014, Nagoya Congress Center, Nagoya, Japan

# Measurement of local plastic deformation in aluminum alloy by means of X-ray 3D imaging technique

Masakazu Kobayashi[a,*], Yuuki Kawamura[a], Soutaro Ueno[a], Hiroyuki Toda[b], Hiromi Miura[a]

[a]*Toyohashi University of Technology, 1-1 Hibarigaoka Tempaku-cho, Toyohashi, Aichi 441-8580, Japan*
[b]*Kyushu University, 744 Motooka Nishi-ku, Fukuoka, Fukuoka 819-0395, Japan*

**Abstract**

To understand the local deformation behavior is very important for improvement of deformability in aluminum alloys which possess poor deformation limit in comparison with steels. However, measurement of local deformation in the interior of metal is not sufficiently carried out. In this study, the development of local plastic strain is measured by means of X-ray 3D imaging technique, i.e. high-resolution synchrotron X-ray microtomography. The marker tracking method, which is based on 3D image processing in volumetric image, is developed for obtaining local strains in 3D. Deformation behaviour is particularly different in individual grains. It was found that grains with different orientations deform maintaining harmony by shear deformation.


Selection and peer-review under responsibility of the Department of Materials Science and Engineering, Nagoya University

*Keywords:* Aluminum alloy; Inhomogeneous deformation; Microtomography; Synchrotron radiation

## 1. Introduction

It is well known that the most fundamental mechanism of plastic deformation in metallic materials is slip deformation. However, development of local inhomogeneous deformation is necessary to accommodate the

* Corresponding author. Tel.: +81-532-44-6706; fax: +81-532-44-6697.
*E-mail address:* m-kobayashi@me.tut.ac.jp


Selection and peer-review under responsibility of the Department of Materials Science and Engineering, Nagoya University
doi:10.1016/j.proeng.2014.10.165

deformations of the individual grains with different crystallographic orientations. Formability of metal rolled sheet changes depending on the statistical deviation of orientation, i.e. crystallographic texture. Crystal plasticity models to predict sheet formability and texture development have been proposed by many researchers. The most classical and famous models is Taylor model (Taylor, 1938). The Taylor model has been extended by Bishop and Hill (1951). The predictions produced by Taylor model are generally analogous with actual textures developed. However, the model exhibits a tendency in which texture becomes sharper than that in experiment. Taylor model assumes that grains deform homogeneously with the strain identical to the global deformation in order to keep continuous strain condition. That is why, various modified models that incorporate an effect of local deformation have been proposed up to today, for example Honneff et al. (1978) and Hamada et al. (2009). Although these modified models could predict texture successfully, we have not particularly understood local deformation in the level of grain microstructure. To understand this local deformation behavior is very important for improvement of deformability in aluminum alloys which possess poor deformation limit in comparison with steels. However, measurement of the local deformation behavior in the interior of metal is not sufficiently carried out. In the present study, the development of local plastic strain is measured by means of X-ray 3D imaging technique, i.e. high-resolution synchrotron X-ray microtomography (Toda et al., 2004, 2011). Inhomogeneous deformation in grain microstructure in aluminum alloy is investigated using this technique. Especially, the variation of deformation was measured for each grain.

## 2. Experiment

### *2.1. Sample*

The aluminum alloy used in this study is heat-treated 2024 aluminum alloy. Large-size grains and spherical precipitates on grain boundaries are obtained by heat-treatment. The grain sizes are about 100-150 μm on rolling plane and about 30-80 μm on the cross section of roll normal direction. The size of precipitates is approximately 3-8 μm. Match-stick-like tensile specimens, which observation part go in field of view (ϕ948 μm × 626 μm), were cut from the sheet by electrical discharge machining. The dimension of the specimen is 0.6 mm × 0.6 mm cross section and 19 mm gage length.

### *2.2. Synchrotron radiation experiment*

Synchrotron radiation experiment was performed at beamline BL47XU and BL20XU in Japanese synchrotron radiation facility, SPring-8. X-ray energy was 20 keV considering a linear absorption coefficient in aluminum alloy.

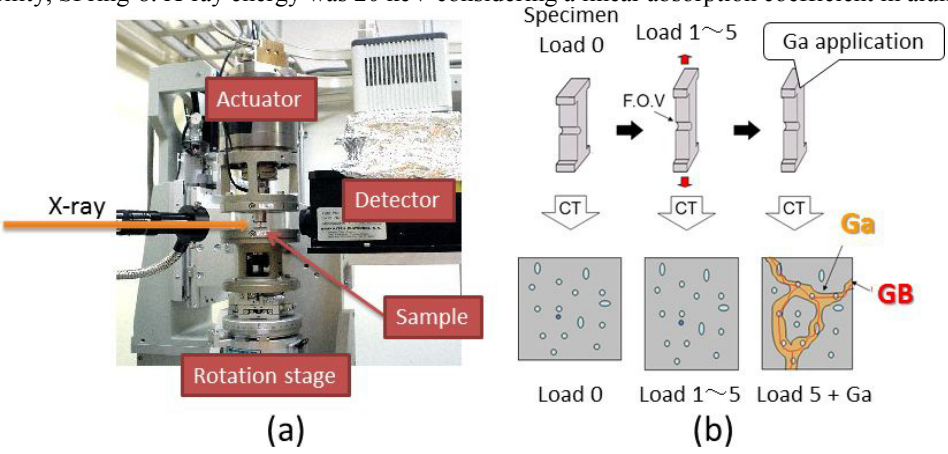


Fig. 1. Synchrotron radiation experiment: (a) set-up of microtomography; (b) procedure of in-situ test.

Small material testing rig, which was designed for SPring-8 beamline and was driven by compression air, was installed in high-accuracy rotation stage as shown in Fig. 1(a). Prepared specimens were set up to the testing rig. The distance of 55 mm between sample and detector was used to enhance image by phase contrast. The detector system consists of a cooled CCD camera (Hamamatsu photonics, C4880-41S: focus = 105 mm, 4000 × 2624 pixels, 5.9 μm × 5.9 μm, 2 × 2 binning mode), an optics lens (× 20) and a scintillator ($Lu_2SiO_5:Ce^+$). A pixel size of detector system was $(0.5\ \mu m)^2$ from the combination of CCD camera and optics lens. The sample was scanned by taking 1500 radiographies from 0 to 180 degree with a 0.12 degree step. The scanning time was about 30 minutes. Schematic illustration of experimental procedure is shown in Fig. 1(b).

Firstly, tomographic scan was performed at non-load situation (Load 0). After that, load was applied to the specimen step by step. The scan was conducted from Load 1 to Load 5 (about the Load 1 to Load 5, it is precisely described in section 3). Before fracture occurs, we stopped increase in loading. Liquid gallium, which preferentially penetrates along aluminum grain boundary, was applied to the tensile deformed specimen. And then tomographic scan was performed again to visualize grain boundary positions. While X-ray diffraction method to enable detection grain boundary position, which is proposed by Poulsen (2004), was not employed because of more simple and easier present method.

### *2.3. Image analysis*

Convolution back projection method as mentioned by Herman (1980) was used for reconstruction of three-dimensional image. The voxel size of reconstructed volumetric image was $(0.5\ \mu m)^3$. Grains in three-dimension were extracted from reconstructed tomography (CT) image obtained after gallium application (doping), which makes grain boundary position clear, by using 3D image processing. Registration was performed between CT images before and after gallium application. This process includes an image contraction of sample that was expanded by gallium penetration into grain boundaries. A part of gallium, which corresponds to grain boundary, was taken out from gallium-applied image by binarization. However, not all grain boundaries can be detected by the binarization. Grain boundary images became occasionally disconnected. Sometimes, particles that have high linear absorption value as similar to gallium were also picked up. So, grains were detected by applying the image processing as follows. (1) Binarized objects that are a volume less than 1000 voxel were removed as a noise. (2) Gray level image that indicates distance from binarized object was produced by the distance transformation. (3) The local minimum was adjusted by the H-minima transformation. (4) Grain area was segmented by Watershed transformation. The details of this procedure have been mentioned by Toda et al. (2013). The number of 74 grains was visualized in this study. Grain that was cut into pieces with (1)-(4) process was merged into one, and then volume and position of gravity center were re-calculated.

### *2.4. Estimation of local plastic strain within grains*

3D strain components of individual grains are estimated from displacement of particles that exist in the detected grain area. A grain contains the number of 10 - 100 particles. The displacement of these particles was measured by tracking them backward from load 5. The matching parameter method proposed by Kobayashi et al. (2008) was utilized for the particles tracking. The weight parameters for distance, volume and surface area were set up as $\alpha$: $\beta$: $\gamma$ = 0.8: 0.1: 0.1. The space within a grain divided into many tetrahedrons, whose vertex is gravity center position of particle, by utilizing 3D Delaunay tessellation algorithm. Strain of a tetrahedron was calculated from displacements of particles that constitute the tetrahedron. The tensile strain in the whole sample was measured from the number of slice by counting 1 pixel as 0.5 μm.

## 3. Result and discussion

The global strain along the tensile direction in Load 1, 2, 3, 4 and 5 was 0.94 %, 1.89 %, 3.52 %, 5.32 % and 8.32%, respectively. Fig. 2 shows maps of strain components in 8.32% global strain (Load 5). Inhomogeneous strain concentration and dispersion are seen in Fig. 2 due to polycrystal grain microstructures. Distribution of strain

components in the Fig. 2 is shown in Fig. 3. Gaussian-type distributions are confirmed both in normal strain and shear strain. In the normal strains, the distributions of $\varepsilon_x$, $\varepsilon_y$ and $\varepsilon_z$ shifted with increasing global tensile strain. However, shape of the distributions did not change with tensile deformation. Average strains calculated from the local strain of $\varepsilon_x$, $\varepsilon_y$ and $\varepsilon_z$ are -2.1 %, -3.6% and 6.0 %, respectively. The average of $\varepsilon_z$ roughly corresponds to global strain of 8.32% along tensile direction in Load 5. Average strain of shear components $\gamma_{xy}$, $\gamma_{yz}$ and $\gamma_{zx}$ are almost zero. In addition, the distribution of shear strain almost is constant during tensile deformation.

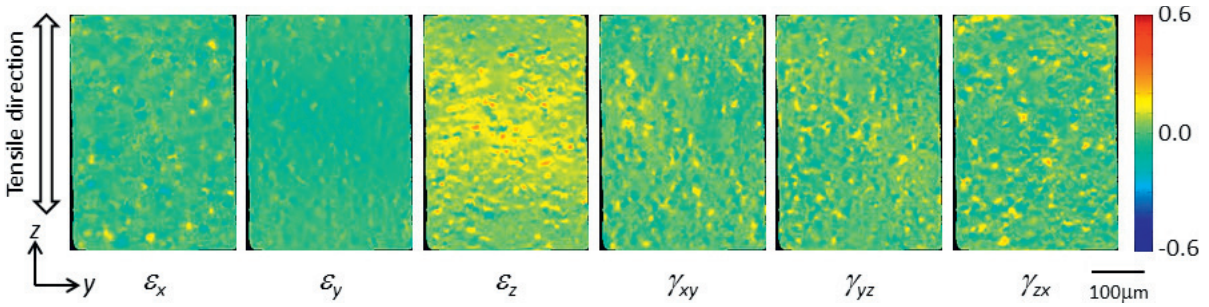


Fig. 2. Strain distribution maps in 8.32 % global tensile strain (Load 5).

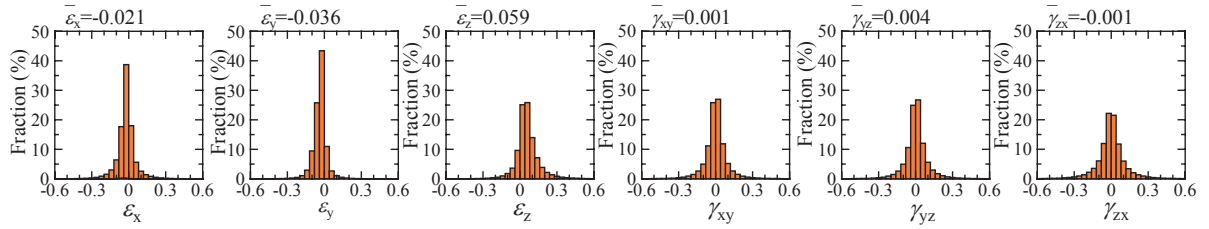


Fig. 3. Distribution of strain components in the whole sample in 8.32 % global tensile strain (Load 5).

A part of result brought by image analysis mentioned in section 2.3 is shown in Fig. 4. Slice image that visualize microstructure by gallium application is indicated in Fig. 4(a). Somewhat elongate grains along the tensile direction are found in microstructure due to roll process. Although some grains are over-partitioned by Watershed transformation, we can confirm segmented grains successfully in Fig. 4(b). 3D view of the segmented grains is shown in Fig. 4(c). Seven aggregated grains are found in this figure.

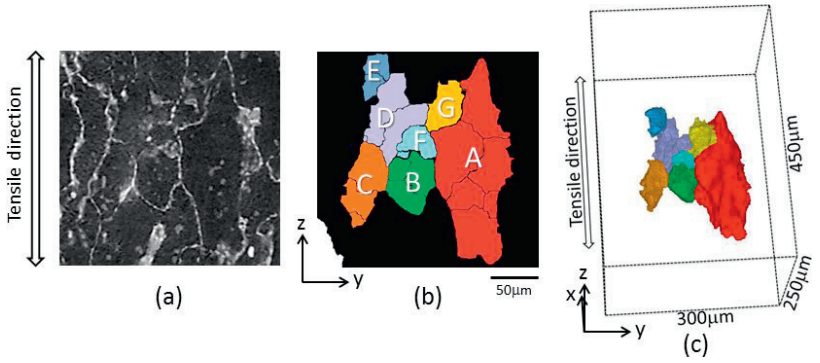


Fig. 4. Result of image analysis: (a) slice image visualized microstructure by gallium application; (b) slice image after Watershed transformation; (c) 3D view of segmented grains.

Strain components in seven grains appeared in Fig. 4 are listed in Table 1. The strains were calculated by taking average of the measured strains within individual grain. The table indicates results in 8.32% global strain (Load 5). Normal strains $\varepsilon_z$, which is strain along tensile, scatter from 1.4% to 11.7%, while global tensile strain is 8.32%. Compression strains of $\varepsilon_y$ are larger than that of $\varepsilon_x$. Every $\varepsilon_x$ strains are very small. This is because x-direction is the normal direction in the rolled sheet. With regard to shear strain, a few percent of shear strain are observed in each grain. It is surmised that behaviors of shear deformation are strongly affected by mechanical properties of neighbor grains. Relatively small scattering was confirmed in $\gamma_{zx}$, in comparison with $\gamma_{xy}$ and $\gamma_{yz}$. However, there was no tendency that neighbor grains deform to the same shear direction. It is suggested that each grain deforms keeping boundary condition with neighbor grains and canceling shear-deformation. Direction of shear deformation seems to be different in individual grains. Therefore, the ratio of shear direction distinguished by plus and minus sign was investigated in the unit of grain. The ratios of shear deformation with plus sign were 41.9 %, 60.8 % and 47.3 % in $\gamma_{xy}$, $\gamma_{yz}$ and $\gamma_{zx}$, respectively. As for the shear strain in $\gamma_{zx}$, the ratio of plus and minus sign was almost half-and-half. However, some deviation was observed in the shear $\gamma_{xy}$ and $\gamma_{yz}$. In addition, relatively small scattering was confirmed in $\gamma_{zx}$. In contrast, tendency of large scattering was observed in $\gamma_{xy}$ and $\gamma_{yz}$. This also seemed to be related with pan-cake like grain microstructure caused by a rolling in sample production process. The z-x plane corresponds to rolling plane, and then grain size is somewhat large.

Table 1. Strain components in the neighboring grains under 8.32% global strain (Load 5).

| | $\varepsilon_x$ | $\varepsilon_y$ | $\varepsilon_z$ | $\gamma_{xy}$ | $\gamma_{yz}$ | $\gamma_{zx}$ |
|---|---|---|---|---|---|---|
| Average in all grains | -0.021 | -0.036 | 0.059 | 0.001 | 0.004 | -0.001 |
| Grain A | -0.044 | -0.063 | 0.117 | 0.022 | 0.019 | -0.002 |
| Grain B | -0.013 | -0.061 | 0.082 | -0.001 | 0.009 | -0.028 |
| **Grain C** | **-0.012** | **-0.050** | **0.063** | **-0.033** | **0.007** | **-0.004** |
| Grain D | -0.024 | -0.075 | 0.060 | -0.054 | 0.011 | -0.002 |
| Grain E | -0.010 | -0.051 | 0.051 | -0.056 | -0.007 | 0.002 |
| Grain F | -0.001 | -0.093 | 0.014 | -0.079 | -0.034 | 0.020 |
| **Grain G** | **-0.021** | **-0.056** | **0.112** | **0.011** | **-0.017** | **0.012** |

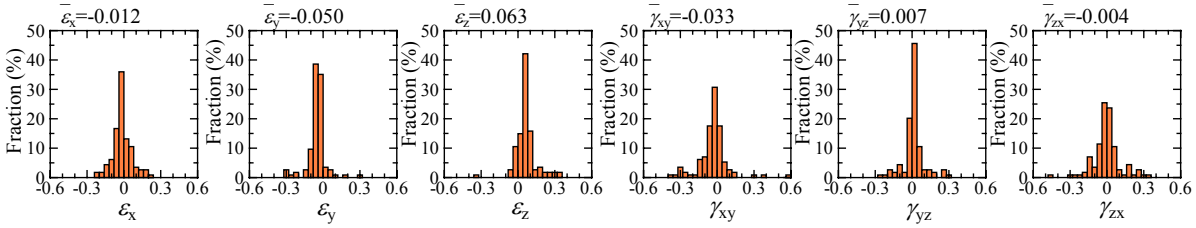


Fig. 5. Distribution of strain components in Grain C.

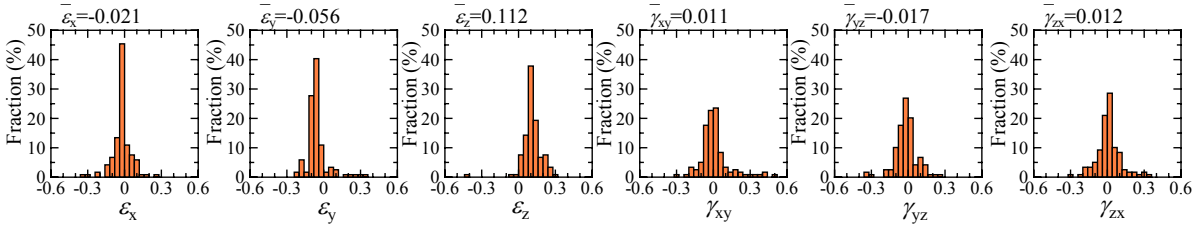


Fig. 6. Distribution of strain components in Grain G.

Distributions of strain components in Grain C and Grain G are shown in Figs. 5 and 6. Number of strain measurement points is 114 and 119 in Grain C and Grain G, respectively. The distributions in individual grain

seem to scatter slightly depending on neighbor grains, though the distribution in whole sample is consistent with Gaussian-type distributions. In both grains, normal strains $\varepsilon_z$ distribute widely in right hand side. Difference of shear strain $\gamma_{yz}$ is noticeable. The other components indicate similar tendency, however, distribution width in grain G seem to be broader than that in Grain C. As shown in here, X-ray 3D imaging technique can measure the development of local plastic strain. We were able to confirm difference of local strain within individual grains. Further analysis and comparison of microstructures, such as crystallographic grain orientation, would help understanding of local deformation behavior.

## 4. Conclusion

Inhomogeneous deformation in grain microstructure in aluminum alloy was investigated using synchrotron radiation microtomography. The variation of deformation and local strain was successfully measured for each grain. The shape of strain distributions didn't change in all strain components with increasing macroscopic tensile strain. With regard to individual grains, local deformation was characterized well. In the sample in this study, relatively smaller scattering in comparison with $\gamma_{xy}$ and $\gamma_{yz}$ was confirmed in shear strain $\gamma_{zx}$ in averaged within a grain. This seemed to be related with pan-cake like grain microstructure caused by a rolling in sample production process. There was no tendency that neighbor grains deform to the same shear direction. It is suggested that each grain deforms keeping boundary condition with neighbor grains and canceling shear-deformation.

## Acknowledgements

The synchrotron radiation experiments were performed with the approval of JASRI through proposal Nos. 2005B0019 and 2007B1213. Authors thank K. Uesugi, A. Takeuchi and Y. Suzuki in JASRI for helping SR experiment. This work was undertaken partly with the support of a Grant-in-Aid for Scientific Research from JSPS through subject No. 24226015. The authors also thank the Light Metal Educational Foundation for support.

## References

[1] Taylor G. I., 1938, Plastic Strain in Metals, J. Inst. Metals, 62, 307-324.
[2] Bishop J. F. W. and Hill R., 1951, A theory of the plastic Dislocation of a Polycrystalline Aggregate under Combined Stresses, Phil. Mag., 42, 414-427.
[3] Bishop J. F. W. and Hill R., 1951, A Theoretical Deriveration of the Plastic Properties f A Polycrystalline Face-Centered Metal, Phil. Mag., 42, 1298-1307.
[4] Honneff H. and Mecking H., 1978, Proc. 5th Int. Conf. in Texture of Materials, ed. by G. Gottstein and K. Lücke, Springer-Verlag, Berlin, 1, 832-842.
[5] Hamada J., Agata K. and Inoue H., 2009, Estimation of Planar Anisotropy of the r-Value in Ferritic Stainless Steel Sheets, Mater. Trans., 50 , 752-758.
[7] Toda H., Maire E., Yamauchi S., Tsuruta H., Hiramatsu T., Kobayashi M., 2011, In situ observation of ductile fracture using X-ray tomography technique, Acta Mater., 59, 1995-2008.
[8] Toda H., Sinclair I., Buffière J. -Y., Maire E., Khor K.H., Gregson P., Kobayashi T., 2004, A 3D measurement procedure for internal local crack driving forces via synchrotron X-ray microtomography, Acta Mater., 52, 1305-1317.
[9] Poulsen H. F., 2004, Three-Dimensional X-Ray Diffraction Microscopy, Springer-Verlag, Berlin Heidelberg.
[10] Herman G. T.,1980, Fundamentals of Computerized Tomography: Image Reconstruction from Projection, Academic Press, New York.
[11] Toda H., Ohkawa Y., Kamiko T., Naganuma T., Uesugi K., Takeuchi A., Suzuki Y., Kobayashi M., 2013, Grain boundary tracking technique: four-dimensional visualisation technique for determining grain boundary geometry with local strain mapping, Acta Mater., 61, 5535-5548.
[12] Kobayashi M., Toda H., Kawai Y., Ohgaki T., Uesugi K., Wilkinson D. S., Kobayashi T., Aoki Y., Nakazawa M., 2008, High-density three-dimensional mapping of internal strain by tracking microstructural features, Acta Mater., 56, 2167-2181.